RSC Advances

ROYAL SOCIETY OF CHEMISTRY

PAPER

View Article Online
View Journal | View Issue



Cite this: *RSC Adv.*, 2020, **10**, 13830

# Synthesis of anti-photolysis lignin-based dispersant and its application in pesticide suspension concentrate

Ruifen Peng,[a] Yuxia Pang,[a] Xueqing Qiu,[ab] Yong Qian[a] and Mingsong Zhou*[a]

Received 17th December 2019
Accepted 18th March 2020

DOI: 10.1039/c9ra10626j

rsc.li/rsc-advances

In the formulation of pesticide Suspension Concentrate (SC), some photosensitive pesticides are easily decomposed in the preparation. In this study, a hindered amine modified lignosulfonate (SL-Temp) with anti-photolysis function was synthesized using 4-amino-2,2,6,6-tetramethylpiperidine (Temp) and Sodium Lignosulfonate (SL) to solve this problem. The obtained SL-Temp was used as a dispersant to prepare 5% SC of avermectin, which shows good physical stability. The decomposition rate of the avermectin in SC after accelerating hot storage is 0%, which is much lower than 6.1% when SL was used as the dispersant. After being exposed to UV irradiation for 60 hours, the highest retention rate of avermectin is 87.1% when SL-Temp was used as the dispersant, which is much higher than 73.6% when SL was used as the dispersant, and also higher than 76.3% when a small molecule antioxidant (BHT) was added to the formulation. QCM-D studies revealed that the SL-Temp adsorption layer on avermectin particles can compete to absorb partial ultraviolet rays, hinder the penetration of ultraviolet light, and scavenge the free radicals produced by photooxidation, so as to protect avermectin from degradation.



## 1. Introduction

The photochemical reaction of pesticides is one of the main ways to degrade pesticides in the atmosphere, and surface water, and on the soil surface and plant surface. Pesticides can be transformed into other non-toxic or less toxic substances by photooxidation, photoreduction, photohydrolysis, molecular rearrangement and isomerization.[1] However, for some photosensitive pesticides, too fast photolysis on the target will lead to a significant decrease in efficacy, which is not conducive to crop protection.[2] Therefore, the photolysis of pesticides has been perplexing the pesticide preparation industry.

Studies have shown that the photolysis of pesticides is hindered by some natural polymer organic compounds. For example, humic acid can reduce the photodegradation rate of fipronil in water, which may be due to the competitive absorption of light by humic acid.[3] Natural compounds such as β-carotene have a photostabilizing effect on pyrethroids pesticides with the mechanism of oxygen consumption competition and photoabsorption competition. The former is that β-carotene is oxidized by dissolved oxygen in solution so that pyrethroid can be protected, and the latter is that β-carotene absorbs incident light and shields pyrethroids.[4] Tea polyphenols have a dual mechanism of photosensitizers and inhibitors on chlorpyrifos pesticide. The former is caused by the external environment to stimulate the production of their own hydroxyl radicals and promote the photolysis of chlorpyrifos. The latter may be due to quenching/antioxidant reduction or hindrance to the photolysis of chlorpyrifos.[5,6] The small molecule antioxidant 2,6-di-*tert*-butyl-4-methylphenol (BHT) has the effect of photostability on avermectin, which may be related to the fact that oxidation is the main photolysis mechanism of avermectin.[7] Therefore, it can be seen that natural polymers containing some chromogenic or reducing groups are beneficial in inhibiting the photolysis of pesticides.

Lignin, as the natural polymer containing polyphenol structure and various chromogenic groups, has the function of scavenging free radicals and antioxidant property.[8] It has been used as a potential antioxidant in polymer, pesticide and other fields.[9,10] Li *et al.* used modified lignin as drug-loaded material, which has a good photostable effect on avermectin. Its action mechanism is that phenolic hydroxyl groups and conjugated carbonyl groups of lignin have scavenging effect on free radicals excited by ultraviolet light and protect avermectin.[11] Yu *et al.* used a one-step hydrothermal esterification reaction to prepare lignin-modified titanium dioxide composite nanoparticles (LS@$TiO_2$), which were applied as the sole active in the pure sunscreen cream. The results show that the sun protection factor (SPF) values of the creams containing 5, 10, and 20 wt% LS@$TiO_2$ are 16, 26, and 48, which are 30–60% higher than those of the creams containing the same amount of $TiO_2$.[12] Deng *et al.* used lignin azo polymer to encapsulate avermectin

[a]*School of Chemistry and Chemical Engineering, Guangdong Engineering Research Center for Green Fine Chemicals, South China University of Technology, Guangzhou 510641, China*

[b]*School of Chemical Engineering and Light Industry, Guangdong University of Technology, Guangzhou 510006, China*

and the encapsulation efficiency of colloidal spheres to avermectin is up to 61.49%. The decomposition rate of avermectin is less than 41% even after 72 hours of UV irradiation.[13] Qian *et al.* used lignin colloidal spheres and pure skin cream *via* physical blending to develop lignin-based sunscreen cream. The results show that the creams blended with lignin colloidal spheres have better sunscreen performance than those blended with original lignin, and the SPF value of the creams decreases with the particle size of lignin colloidal spheres.[14] However, from the previous studies, it is also found that the phenolic hydroxyl group content of lignin is limited and the antioxidant activity is weak, so it is not an efficient photostable compound.[15–17]

Pesticide Suspension Concentrate (SC) is a kind of water-based environmental protection formulation obtained by wet grinding of water-insoluble solid pesticides and dispersing agents, stabilizer and other auxiliaries with water as dispersion medium. It is a fashionable formulation in accordance with the concept of environmental protection.[18,19] However, compared to Emulsifiable Concentrate (EC) formulation and solid formulations (*e.g.*, wettable powder and water dispersible granule), due to the presence of water in the formulation, SC is more easily decomposed by photooxidation during storage and application, and the chemical stability of the formulation is more difficult to maintain.

In this study, Sodium Lignosulfonate (SL) was used as raw material to prepare an anti-photolysis lignin-based dispersant by introducing tetramethylpiperidine (Temp) into SL molecule, and it was used in the preparation of 5% avermectin SC. Furthermore, its photostabilization and related mechanism was studied in detail.

## 2. Experimental

### 2.1. Materials

SL is a purified product from poplar acid pulping effluent, provided by Shixian Paper-making Co., Ltd. (Jilin, China). The original avermectin powder (95.5% purity) is provided by the Noposion Agrochemical Co., Ltd (Shenzhen, China), the structure is shown in Fig. 1. The xanthan gum is provided by Zhiyuan Chemical products Co., Ltd. (Henan, China). The magnesium aluminum silicate is provided by Boshuo Technology Co., Ltd. (Anhui, China). The other chemicals including formaldehyde (36% purity), 4-amion-2,2,6,6-tetramentylniperidine, BHT, ethanol, ethylene glycol, Nekal BX are all analytical grades, provided by Aladdin chemical reagents Co., Ltd. (Shanghai, China). The experiment water is deionized water.

### 2.2. Preparation of SL-Temp

Firstly, 10 g SL was dissolved in 40 g deionized water, and the pH of SL solution was adjusted to 10–12 using NaOH solution (30%, w/w). Then, a certain amount of Temp was added to the SL aqueous solution and kept stirring for 15 minutes at 70 °C. Finally, the diluted formaldehyde solution (10%, the molar ratio of formaldehyde to Temp was 1.1 : 1) was dripped into the mixture at a uniform rate in 30 minutes, and reacted at 85 °C for 3 hours. After cooling down to room temperature, excess ethanol was added to the mixture and the product was precipitated. The precipitated solid products were washed with ethanol for three times, then dried at 45 °C for 24 hours. The obtained dry product is described as SL-Temp. The molecular design and reaction process of SL-Temp is shown in Fig. 2.

### 2.3. Characterizations of SL-Temp

Elemental analyses of the samples were performed on an elemental analyzer (vario EL cube, Germany).

FTIR spectra of the samples were measured on a Vector 333 FT-IR spectrometer (Bruker, Germany). The tested samples were prepared by mixing 1 mg dried samples with 50 mg KBr and then was pressed under 8 MPa for 30 seconds.

$^1$H-NMR spectra of the samples were performed by an Advance Digital 400 MHz NMR spectrometer (Bruker, Germany). The tested samples were prepared by dissolving 30 mg dried samples in 0.5 mL DMSO-$d_6$, the obtained solutions were used for $^1$H-NMR characterization.

Electron Paramagnetic Resonance (EPR) spectra of samples were recorded by ELEXSYS-II E500 spectrometer (Bruker, Germany). The range of the test magnetic field is 2000–5000 mT, the test frequency band is X-band, and the test power is 2 mW.

### 2.4. Preparation of SC

The 5% avermectin SC was prepared by wet grinding with a vertical bead mill (B06334, Shenyang Institute of Chemical Industry, China) and some zirconium balls with a diameter of 0.3 mm. The materials were prepared according to the formulation in Table 1, and the 5% avermectin SC was obtained by

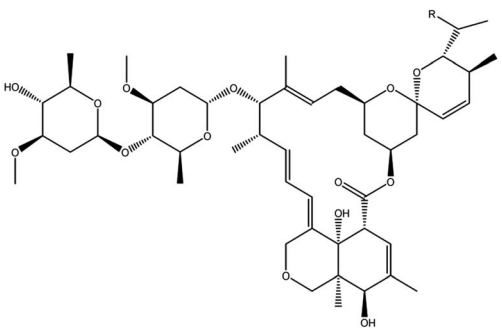

Fig. 1 The chemical structure of avermectin.

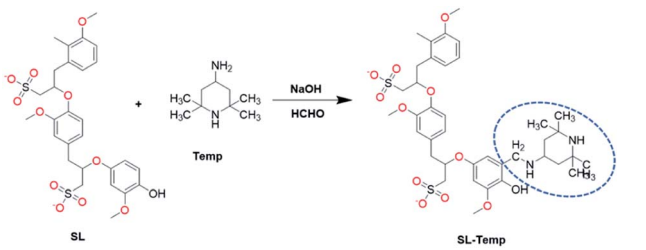


Fig. 2 The molecular design and reaction process of SL-Temp.

Table 1 The formula of 5% avermectin SC[a]

| Component | Reagent | Dosage (%) |
|---|---|---|
| Pure drug | Avermectin (purity 92.2%) | 5.3 |
| Dispersant | SL or SL-Temp | 3.0 |
| Wetting agent | Nekal BX | 0.5 |
| Static stabilizer | Magnesium aluminium silicate solution | 40.0 |
| | Xanthan gum solution | 8.0 |
| Antifreeze agent | Ethylene glycol | 3.0 |
| Defoamer | Organic silicon | 0.5 |
| Medium | Water | Add to 100 |

[a] Before grinding, the magnesium silicate and xanthan gum should be dissolved in water to obtain 2.5% swelling solution for use.

grinding at room temperature for 2 hours. The pH value of the SC was adjusted to 7 by adding HCl/NaOH (0.1 mol $L^{-1}$).

### 2.5. Determination of performance of SC

The zeta potential on the surface of pesticide particles in SC was measured by zeta potential tester (ZS Nano S, Brookhaven, American). The SC was diluted in deionized water to prepare 1 g $L^{-1}$ solution, then the average value was obtained after three parallel measurements.

The particle size distribution of SC was tested by an MS2000 laser diffraction particle size analyzer equipped with a Hydro SM wet dispersion unit (Malvern Instruments, U.K.). 0.1 g SC was dispersed in 50 mL deionized water, then tested at 2000 rpm, and the average value was obtained after three parallel measurements.

The stability of SC was tested through an accelerated test of hot storage. The SC was sealed in clean brown vials in a UNE400 incubator (Memmert, Germany) and placed at 55 ±1 °C for 14 days, then the particle size distribution and the effective avermectin content of the samples were determined after hot storage.

The suspension rate of avermectin SC was performed according to Chinese National Standard Method GB/T14825-2006. The content of active ingredient in the SC was tested by a high-performance liquid chromatography (HPLC, LC-20A, Japan). 1.0 g SC was dispersed into 250 mL plug cylinder with standard hard water. According to the national standard, the mass of the active ingredient in the 25 mL suspension at the bottom of the cylinder was determined, the average value was obtained after three parallel measurements, and the suspension rate A (%) was calculated by formula (1).

$$A = 10 \times (M_1 - M_2)/(9 \times M_1) \times 100\% \quad (1)$$

Among them, $M_1$ is the mass of the active ingredient in the sample (g) and $M_2$ is the mass of the active ingredient in the 25 mL suspension at the bottom of the cylinder.

### 2.6. Photodegradation study

The anti-photolysis performance of avermectin SC was evaluated by film method. First, 1.0 g SC was diluted into a 100 mL volumetric flask. Then, extracted 400 μL diluent and evenly spread on a 3.5 cm diameter glass Petri dish and dried into a thin film at the room temperature. These films were exposed to UV light (30 W, 310 nm) for 0, 10, 20, 30, 40, 50, 60, 70 hours. The remaining avermectin in each film was dissolved by using 5 mL methanol and then was detected by HPLC.

### 2.7. Determination of adsorption property

The adsorption property of SL and SL-Temp on gold-coated quartz crystal ($QC_{gold}$, the fundamental frequency is 5 MHZ) treated with a coated layer of avermectin was determined by means of a quartz crystal microbalance instrument (Q-SenseE1, Q-Sense AB Corp., Sweden). Prior to the adsorption of SL and SL-Temp, the $QC_{gold}$ was immersed in a 5 : 1 : 1 mixture of water, $H_2O_2$ (30%), and $NH_4OH$ (25%) for 5 minutes and rinsed with ethanol for 10 minutes, then dried under $N_2$ stream. Subsequently, the avermectin ethanol solution (0.1 mg $mL^{-1}$) was uniformly coated on the $QC_{gold}$ by a spin coater (AC200, Jiatu Technology Co., Ltd, China) and kept in a cool place to evaporate solvent. Then the coated $QC_{gold}$ was embedded in the instrument for measurement. The concentration of sample solutions was 500 mg $L^{-1}$, and the pH value was adjusted to 7. The $QC_{gold}$ was initially rinsed in deionized water until a stable baseline was established before rinsing in sample solutions. The velocity of the peristaltic pump was maintained at 0.15 mL $min^{-1}$, and the frequency changes ($\Delta f$) and dissipation ($\Delta D$) of $QC_{gold}$ were monitored.

## 3. Results and discussion

### 3.1. Characterizations of SL-Temp

In the Mannich graft reaction of lignin, the grafting amount of the Temp group in the product can be directly affected by the amount of hindered amine monomer.[20] The SL-Temps with different Temp group contents were obtained by changing the mass ratio of Temp to SL (Temp/SL = 10, 20, 30 wt%), and the products are described as SL-$Temp_1$, SL-$Temp_2$ and SL-$Temp_3$, respectively. The elemental analysis of different SL-Temp samples are shown in Table 2.

Because N element is the characteristic element of Temp functional group, and the content of N element in SL is very low, the content of Temp group in the modified product can be calculated from the content of N element. As shown in Table 2,

 

Table 2 Elemental analysis of different SL-Temp samples

| Samples | Elemental Content (%) | | Temp Content (%) | | Sulfonation degree (mmol $g^{-1}$) | Grafting efficieny (%) |
|---|---|---|---|---|---|---|
| | N | S | wt% | mmol $g^{-1}$ | | |
| SL | 0.11 | 5.55 | — | — | 1.73 | — |
| SL-Temp$_1$ | 1.84 | 5.01 | 7.29 | 0.62 | 1.57 | 78.63 |
| SL-Temp$_2$ | 2.36 | 4.90 | 12.48 | 0.80 | 1.53 | 71.30 |
| SL-Temp$_3$ | 3.35 | 4.38 | 17.97 | 1.16 | 1.37 | 73.02 |

with the increasing amount of hindered amine monomer, the content of N element increases gradually from 0.11% of SL to 1.84%, 2.36%, and 3.35%. It can be calculated that the content of Temp group in SL-Temp is 0.62 mmol $g^{-1}$, 0.80 mmol $g^{-1}$ and 1.16 mmol $g^{-1}$, respectively. In addition, the sulfonic group content of SL-Temp can be calculated by the content of S element in SL-Temp. It is found that the sulfonic group content in SL decreases slightly with the increase of the Temp grafting rate in SL.

The SL-Temp$_3$ with the highest grafting rate was characterized by infrared spectroscopy, and the results are shown in Fig. 3.

As can be seen from Fig. 3, the peak shape of SL-Temp$_3$ is similar to that of SL, but a new absorption peak appears at 1388 $cm^{-1}$, which is the symmetric bending vibration peak of methyl caused by the vibration coupling of two methyl groups connected to the same carbon atom in Temp. In addition, since Temp contains more methyl and methylene, the symmetric stretching vibration peaks of methylene (C–H) near 2853 $cm^{-1}$ and antisymmetric stretching vibration peaks of methyl (C–H) near 2942 $cm^{-1}$ of SL-Temp$_3$ are enhanced, respectively. From the results of infrared spectroscopy, it can be preliminarily judged that Temp has been successfully grafting into SL.

SL-Temp$_3$ was further characterized by $^1$H-NMR spectra. The results are shown in Fig. 4.

From Fig. 4, the peak at 6.48–7.25 ppm can be attributed to the proton peak on benzene ring, and the signal intensity of SL-Temp$_3$ is weaker than that of SL. It indicates that the H atom on the benzene ring is reduced, which is caused by the substitution reaction of Temp at the ortho position of the phenolic hydroxyl group on the benzene ring. Besides, since Temp contains more methyl and methylene, the peak at 1.0–1.6 ppm, which is attributed to the α-H signal of methyl(–$CH_3$) and methylene(–$CH_2$–), is observed in SL-Temp$_3$. The analysis results of $^1$H-NMR spectra further prove that there are a large number of Temp groups in SL-Temp.

In the presence of ultraviolet irradiation and oxygen, the Temp group introduced into SL is easily converted into a piperidine nitroxide radical (Tempo), which can be detected by electron parammagnetic resonance (EPR).[21] The powder samples of SL and SL-Temp$_3$ were dried and characterized by EPR. The results are shown in Fig. 5.

From Fig. 5, compared with SL, the EPR spectrum of SL-Temp$_3$ has changed obviously. There is an asymmetric dual peak of SL-Temp near $g = 2.00253$, which has the characteristic of typical double radicals.[22] In addition, SL-Temp$_3$ has a stronger signal intensity, which means that more stable Tempo is produced by SL-Temp. This is beneficial to promote the cycle process of scavenging alkyl free radicals.[23] Therefore, the introduction of the Temp group can improve the anti-photolysis ability of SL, and the obtained SL-Temp is a functional polymeric surfactant which can inhibit photodegradation.

The obtained SL-Temps were used as functional dispersant in the preparation of 5% avermectin SC, and the related properties of SC were studied.

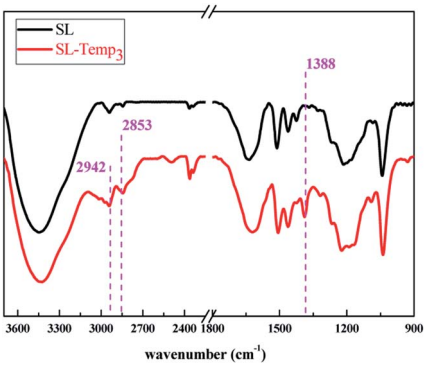


Fig. 3 FT-IR spectra of SL and SL-Temp$_3$.

### 3.2. Effects of SL-Temps with different Temp contents on particle size and zeta potential of SC

The smaller the particle size of SC is, the more beneficial it is to improve the suspension rate and efficacy.[24] According to national standards, the average particle size ($D_{50}$) of SC is usually 2–5 μm.[25] The 5% avermectin SC was prepared using the SL-Temps with different Temp contents as dispersant, and the effects of Temp group content on the particle size and zeta potential of SC were studied. The results are shown in Table 3.

From Table 3, the $D_{50}$ of 5% avermectin SCs prepared by SL-Temps with different Temp contents are all less than 5 μm, which meets the requirements of national standard. The absolute value of zeta potential of the pesticide particles is reduced by SL-Temp, which is intensified with the increasing Temp group content. It is considered that the Temp contains amino group and forms cationic group after ionization in water, which

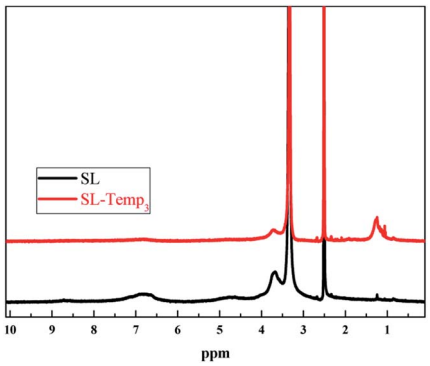


Fig. 4 $^{1}$H-NMR spectra of SL and SL-Temp$_3$.

neutralizes the anion charge of some sulfonic groups. Therefore, the absolute value of zeta potential of particles turns slightly smaller, but this does not affect the dispersion performance of SL-Temp.

### 3.3. Effect of SL-Temps with different Temp contents on hot storage stability of SC

The stability of pesticide SC is of great significance for its long-term storage, including physical stability and chemical stability. The physical stability is mainly characterized by the changes of the particle size and suspension rate, and the chemical stability is characterized by the decomposition rate of the effective ingredient. The avermectin SCs prepared using SL-Temps with different Temp contents as dispersant were stored at 55 °C for 14 days. The hot storage stability is evaluated by the decomposition rate of the effective ingredient, the suspension rate and the particle size change. The results are shown in Table 4.

As is shown in Table 4, the $D_{50}$ of the SCs prepared by SL and the SL-Temps with different Temp group contents remains unchanged after hot storage, and the suspension rates are all above 99%. This shows that the four dispersants have good dispersing ability to 5% avermectin SC, and the physical stability of the SC is excellent. However, the effective avermectin contents in the SC prepared by SL and the SL-Temps with different Temp contents are quite different before and after hot storage. The decomposition rates of avermectin in the SC prepared by SL and SL-Temp$_1$ are 6.1% and 5.9%, respectively, while avermectin in the SC prepared by SL-Temp$_2$ and SL-Temp$_3$ does not decompose obviously after hot storage, and the decomposition rates are 0%. This indicates that the introduction of Temp functional group into SL molecule is beneficial to inhibit the decomposition of avermectin from oxidation during hot storage, and the higher the content of Temp group is, the more significant the inhibitory effect is.

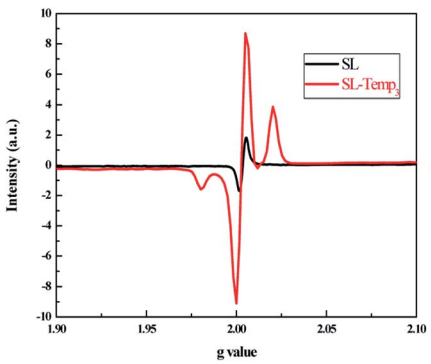


Fig. 5 EPR spectra of SL and SL-Temp$_3$.

Table 3 Zeta potential and average particle size ($D_{50}$) of 5% avermectin SC with different dispersants

| Samples | $D_{50}$/μm | Zeta potential/mv |
|---|---|---|
| SL | 3.01 | −49.7 ± 0.1 |
| SL-Temp$_1$ | 2.94 | −43.0 ± 3.4 |
| SL-Temp$_2$ | 2.96 | −39.3 ± 1.9 |
| SL-Temp$_3$ | 3.14 | −36.4 ± 1.1 |

### 3.4. Effect of Temp contents on adsorption property of SL-Temps on pesticide particles

Quartz crystal microbalance combined with dissipation monitoring (QCM-D), as a tool for quantitative real-time analysis of interface behavior, can monitor the adsorption kinetics and molecular conformation of the dispersant at the interface, and study the adsorption characteristics of dispersant on the surface of pesticide particles. In this study, QCM-D was used to detect the curves of the resonance frequency F and the energy dissipation factor $D$ caused by the adsorption behavior of the SL-Temps with different Temp contents on the surface of avermectin particles. For thin adsorption layers, changes in the resonance frequency ($\Delta f$) represent the adsorption amounts on QC$_{gold}$, the absolute values of which are positively correlated with mass uptake or release at the sensor surface, and changes in the dissipation factor ($\Delta D$) represent the viscoelasticity of the adsorption layer. The experiment was carried out at 25 °C, and the results are shown in Fig. 6.

From Fig. 6(a), according to the absolute values of $\Delta f$, the adsorption amounts of SL-Temp onto QC$_{gold}$ increase with increasing content of the Temp group in SL-Temp. It is considered that the increase of Temp content can enhance the adsorption force between SL-Temp and hydrophobic pesticide surface, which leads to the increase of adsorption capacity. From Fig. 6(b), with the increase of Temp content in SL-Temp, $\Delta D$ increases gradually, so the viscoelasticity of the adsorption film is strengthened, which indicates that the adsorption film of SL-Temp on the avermectin surface is more compact and the adsorption strength is higher. The curves of $\Delta f$ and $\Delta D$ show that the increase of Temp group content is beneficial to increase the adsorption amounts of SL-Temp on avermectin surface and the compactness of the adsorption layer, which is beneficial to the improvement of the dispersing performance of SL-Temp. Meanwhile, the SL-Temp adsorption layer, which is tightly covered on the surface of avermectin particles, can protect avermectin particles from decomposition by hindering the

 

Table 4 Hot storage stability of 5% avermectin SC with different dispersants

| | Before hot storage | | | After hot storage | | | |
|---|---|---|---|---|---|---|---|
| Dispersant | Active ingredient content/% | Suspensibilty/% | Particle size $D_{50}$/μm | Active ingredient content/% | Suspensibilty/% | Particle size $D_{50}$/μm | Decomposition rate of avermectin/% |
| SL | 4.9 ± 0.01 | 99.2 ± 0.46 | 3.06 | 4.6 ± 0.01 | 99.3 ± 0.28 | 2.83 | 6.1 |
| SL-Temp$_1$ | 5.1 ± 0.08 | 100.0 ± 0.99 | 3.00 | 4.8 ± 0.06 | 99.6 ± 1.38 | 2.83 | 5.9 |
| SL-Temp$_2$ | 4.7 ± 0.03 | 99.5 ± 0.31 | 3.00 | 4.7 ± 0.02 | 99.8 ± 0.60 | 3.00 | 0.0 |
| SL-Temp$_3$ | 4.7 ± 0.01 | 99.5 ± 0.02 | 3.17 | 4.7 ± 0.02 | 99.2 ± 0.21 | 3.11 | 0.0 |

penetration of ultraviolet light and scavenging the free radicals generated as much as possible.

### 3.5. Effect of SL-Temps with different Temp contents on anti-photolysis performance of SC

During the spraying process of avermectin SC, the pesticide film sprayed on the leaf surface of the crop is directly exposed to the sun. Without the protection of the light stabilizer, avermectin will be decomposed rapidly by photooxidation, resulting in a significant decrease in efficacy. In order to reduce the photolysis loss of avermectin SC, the formulation engineers usually add a small number of antioxidants, such as small molecule antioxidant BHT, to SC preparations to reduce the photooxidative decomposition of avermectin.

In order to compare the difference of anti-photolysis performance between SL-Temp and BHT, the diluents of the avermectin SC prepared by SL-Temps with different Temp contents were dried into film in the dark, then irradiated under UV light to study the anti-photolysis performance. Meanwhile, the 5% avermectin SC prepared by grinding with BHT (addition amount = 3%) and a phosphate type dispersant 601-P without anti-photolysis ability was used as a control. The results are shown in Fig. 7.

As can be seen from Fig. 7, after 60 hours of ultraviolet light, the effective avermectin contents in SC all decrease, among which the retention rate of avermectin in the SC prepared by SL is the lowest (73.6%). The retention rate of avermectin in the SC with 601P and BHT as additives is 76.3%, which is only slightly higher than that of the SC with SL. Besides, the retention rates of avermectin in the SC with SL-Temps as dispersant increase with the increasing Temp group content. Among them, the retention rate of avermectin in the SC with SL-Temp$_3$ is the highest (87.1%). It shows that SL-Temp can effectively protect the effective avermectin in SC and has obvious anti-photolysis performance, compared with SL. Therefore, the introduction of Temp groups can significantly improve the anti-photolysis performance of lignin-based dispersant. Although the antioxidant component BHT was added to the SC prepared by 601P dispersant, the effect is not so ideal, which is only slightly better than that of the unmodified SL.

At the same addition amount of 3%, why the photostability of SL-Temp for avermectin SC is much better than that of small molecule antioxidant BHT. The photostabilization mechanism of avermectin by SL-Temp is expounded from the point of view of liquid/solid interface adsorption.

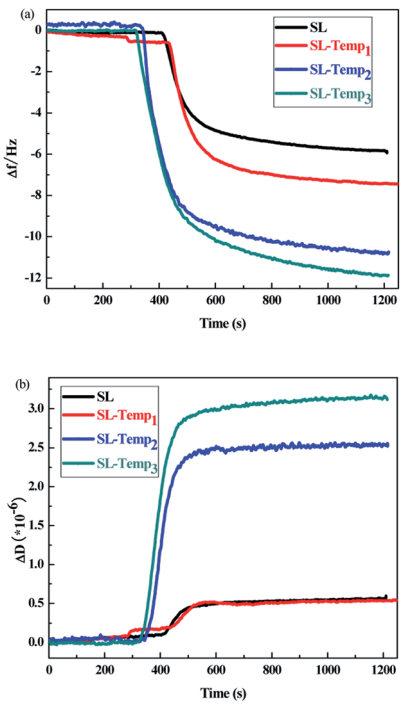


Fig. 6 (a) Δ$f$ adsorption curves of different dispersants on avermectin; (b) Δ$D$ adsorption curves of different dispersants on avermectin.

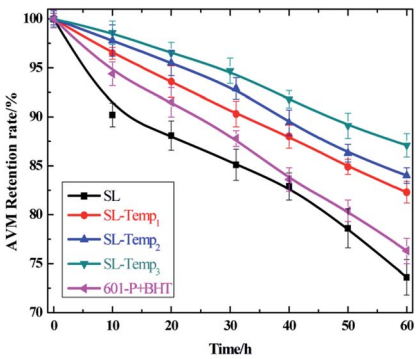


Fig. 7 UV degradation curves of avermectin in the SC with different additives.

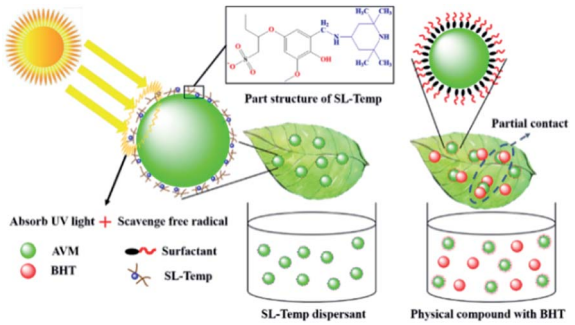


Fig. 8 The anti-photolysis model diagram of the avermectin SC with SL-Temp and BHT additives.

### 3.6. Anti-photolysis mechanism of SL-Temp to avermectin SC

From Fig. 6, in SC, SL-Temp is adsorbed on the surface of avermectin particles in molecular state and the adsorption amounts as well as the compactness of the adsorption layer are greater than SL. However, in the SC prepared by 601-P and BHT, BHT is not soluble in water, but is ground into small particles ($D_{50}$ = 5–7 μm) and uniformly dispersed in the SC with avermectin particles. Therefore, the protective forms of SL-Temp and BHT on avermectin particles in SC are different, and the model diagram of their interaction with avermectin particles is shown in Fig. 8.

As is shown in Fig. 8, in avermectin SC, SL-Temp is tightly adsorbed on the surface of avermectin particles in molecular state, forming a compact adsorption layer. When the SC diluent is sprayed on the target surface, SL-Temp molecules containing antioxidant and light-stabilizing groups are tightly wrapped on the surface of pesticide particles. The phenolic hydroxyl groups, conjugated carbonyl groups and Temp groups in SL-Temp molecules interact with each other when the sun light is irradiated on the surface of the pesticide particles. On the one hand, they compete to absorb most of the incident light to shield the photodegradation, on the other hand, they scavenge the active free radicals generated by photooxidation, thus protecting the internal avermectin particles.

However, in avermectin SC, BHT is uniformly mixed with avermectin particles in the form of particles, and the size of BHT particles is not significantly different from that of avermectin particles, so it is difficult to adsorb closely on the surface of avermectin particles. When SC diluent is sprayed on the target surface, BHT particles do not absorb ultraviolet light, and only partially scavenge the active free radicals produced by photooxidation, thus realizing the weakly protecting effect on avermectin particles. Besides, due to the large size of BHT particles. Therefore, the protecting effect of BHT on avermectin in SC formulation is weaker than that of anti-photolysis polymer dispersant SL-Temp.

## 4. Conclusions

The functional dispersant SL-Temp was prepared using SL and hindered amine monomer. The elemental analysis, FT-IR spectra and $^1$H-NMR spectra prove that the hindered amine monomer has been successfully grafting into SL. The EPR spectrum indicates the obtained SL-Temp is a functional polymeric surfactant which can inhibit photodegradation. The SL-Temp was used as dispersant to prepare 5% SC of avermectin. After 14 days of accelerated experiment of hot storage, the particle size of the SC remains unchanged and the suspension rates are both higher than 99% before and after hot storage, which mean that the physical stability of the SC is good. Meanwhile, the decomposition rate of the avermectin in SC after hot storage is 0%, which is much lower than 6.1% when SL was used as dispersant, indicating that the chemical stability of the SC is good. QCM-D studies show that the introduction of Temp group is beneficial to increase the adsorption amount of SL-Temp on avermectin surface and the compactness of the adsorption layer. The SL-Temp adsorption layer tightly covered on the surface of avermectin particles can protect avermectin particles from decomposition by hindering the penetration of ultraviolet light and scavenging the free radicals generated.

## Conflicts of interest

There are no conflicts to declare.

## Acknowledgements

We gratefully acknowledge the financial support from the National Natural Science Foundation of China (21690083, 21878112), the Natural Science Foundation of Guangdong Province (2020A151501010, 2017A030308012, 2017B090903003) and the Guangdong Provincial Special Fund for Modern Agriculture Industry Technology Innovation Teams (2019KJ140).

## References

1 Y. B. Si, Y. D. Yue, D. M. Zhou and H. M. Chen, *Rural Eco-Environ.*, 2002, **18**, 56–59.
2 L. S. Crouch, W. F. Feely, B. H. Arison, W. J. A. VandenHeuve, L. F. Colwell, R. A. Stearns, W. F. Kline and P. G. Wislocki, *J. Agric. Food Chem.*, 1991, **39**, 1310–1319.
3 S. S. Walse, S. L. Morgan, L. Kong and J. L. Ferry, *Environ. Sci. Technol.*, 2004, **38**, 3908–3915.
4 G. Bi, S. Z. Tian, Z. G. Feng and J. K. Cheng, *Environ. Chem.*, 1995, **5**, 425–430.
5 R. G. Oliver, D. F. Wallace and M. Earll, *Pest Manage. Sci.*, 2013, **69**, 120–125.
6 L. M. Canle, M. I. Fernández and J. A. Santaballa, *J. Phys. Org. Chem.*, 2010, **18**, 148–155.
7 W. J. Song and F. S. Lu, *Mod. Agrochem.*, 2017, **16**, 21–23.
8 Z. Qin, Z. G. Zhang, H. M. Liu, G. Y. Qin and X. D. Wang, *RSC Adv.*, 2018, **8**, 24923–24931.
9 D. Kai, Y. K. Chua, L. Jiang, C. Owh, S. Y. Chan and X. J. Loh, *RSC Adv.*, 2016, **6**, 86420–86427.
10 Z. L. Li and Y. Y. Ge, *Int. J. Biol. Macromol.*, 2012, **51**, 1116–1120.
11 Y. X. Li, M. S. Zhou, Y. X. Pang and X. Q. Qiu, *ACS Sustainable Chem. Eng.*, 2017, **5**, 3321–3328.

 

12 J. Yu, L. Li, Y. Qian, H. M. Lou, D. J. Yang and X. Q. Qiu, *Ind. Eng. Chem. Res.*, 2018, **57**, 15740–15748.
13 Y. H. Deng, H. J. Zhao, Y. Qian, L. Lü, B. B. Wang and X. Q. Qiu, *Ind. Crops Prod.*, 2016, **87**, 191–197.
14 Y. Qian, X. W. Zhong, Y. Li and X. Q. Qiu, *Ind. Crops Prod.*, 2017, **101**, 54–60.
15 A. Arshanitsa, J. Ponomarenko, T. Dizhbite, A. Andersone, R. J. A. Gosslink, J. V. D. Putten, M. Lauberts and G. Telysheva, *J. Anal. Appl. Pyrolysis*, 2013, **103**, 78–85.
16 X. J. Pan, J. F. Kadla, K. Ehara, N. Gilkes and J. N. Saddler, *J. Agric. Food Chem.*, 2006, **54**, 5806–5813.
17 C. Pouteau, B. Cathala, P. Dole, B. Kurek and B. Monties, *Ind. Crops Prod.*, 2005, **21**, 101–108.
18 L. G. Pan, L. M. Tao and X. Zhang, *Plant Prot.*, 2005, **31**, 22–23.
19 A. Knowles, *Environmentalist*, 2008, **28**, 35–44.
20 X. Yue, W. H. Qiao, K. H. Shen and Z. S. Li, *Fine Chem.*, 2001, **18**, 670–673.
21 M. V. Motyakin and S. Schlick, *Macromolecules*, 2002, **35**, 3984–3992.
22 E. A. Haidasz, D. Meng, R. Amorati, A. Baschieri, K. U. Ingold, L. Valgimigli and D. A. Pratt, *J. Am. Chem. Soc.*, 2016, **138**, 5290–5298.
23 Y. P. Liu and J. L. Zweier, *J. Magn. Reson.*, 2010, **27**, 95–102.
24 N. Z. Hua and C. Hua, *World Pestic.*, 2013, **35**, 29–33.
25 S. Haas, H. Hans-Walter and C. Schlatter, *Colloids Surf., A*, 2001, **183**, 785–793.